Doubly Okubo-Zweig-Iizuka-rule–violating effects in J/ψ decays

Abraham Seiden, Hartmut F.-W. Sadrozinski, and Howard E. Haber
Santa Cruz Institute for Particle Physics, University of California, Santa Cruz, California 95064
(Received 17 March 1988)

We analyze some of the existing data available for the hadronic and radiative production of mesons from the J/ψ. A reanalysis of the decays into a pseudoscalar- and vector-meson pair indicates good agreement with the pseudoscalar mixing angle derived from the new two-photon widths of these mesons. An important ingredient is the inclusion of the doubly disconnected diagram, which also provides a natural mechanism for decays into a meson plus gluonium. We attempt to estimate the decay rate of J/ψ into gluonium and mesons using the radiative decay widths as input. We also present a discussion of J/ψ decays into tensor + vector and axial-vector + vector states.

I. INTRODUCTION

Decays of the J/ψ allow a unique study of meson spectroscopy in the 1–2-GeV mass region. One can study quark content, gluonium, effects of SU(3) breaking, electromagnetic amplitudes, and spin-parity for a variety of two-body final states. Of particular importance for an understanding of QCD is the gluonium spectrum. Two such gluonium-candidate states[1-3] are the ι and θ, with spin-parity 0^- and 2^+, respectively.[4] Evidence for such an interpretation of these states comes from the fact that they have large rates in radiative J/ψ decay and appear as single states without partners, unlike the ordinary isoscalar meson pairs of analogous spin-parity: η,η' or f,f'. Dynamical evidence for this interpretation comes from the two-photon reactions where the gluonium states are strongly suppressed relative to the normal mesons and from hadronic J/ψ decays where they are suppressed relative to decays such as $\omega\eta,\phi\eta',\omega f,\phi f'$. The suppression comes about in $\gamma\gamma$ reactions because gluonium states have no charged constituents and in J/ψ decays because the gluonium states suffer an extra Okubo-Zweig-Iizuka (OZI) suppression[5] in the hadronic decays. The dynamical evidence, however, requires that we understand the mixing pattern of gluonium with the normal mesons as well as the degree of suppression coming from the OZI rule. J/ψ decays provide a unique source for studying these issues.

The prototype of such a study is the Mark III analysis of $J/\psi\to P+V$ (pseudoscalar+vector meson) final states.[6-8] The conclusions of that analysis, that there may be substantial $\eta'-\iota$ mixing, are in conflict[9] with the new two-photon widths for the η,η',ι. As pointed out by Pinsky,[10] the principal inadequacy of the Mark III analysis is the assumption that the decays proceed via the singly disconnected (SOZI) diagram [Fig. 1(a)] alone, while omitting the doubly disconnected (DOZI) diagram [Fig. 1(b)]. In group-theoretical language, the existence of DOZI contributions corresponds to nonet symmetry breaking. A small DOZI amplitude can produce a large effect because of interference with the larger SOZI amplitude.

Evidence for the importance of the DOZI amplitude is the decay $J/\psi\to\gamma+\text{vector}+\text{vector}$. This process shows a clear DOZI decay in that the rate for $\gamma+\omega\phi$ does not vanish.[11] The rates are given in Table I, and they indicate that the DOZI amplitude is ~ 0.3–0.5 of the allowed (singly disconnected or SOZI) amplitude for this channel. In this paper we reconsider the $P+V$ decays, including the DOZI contribution. The new two-photon data[12,13] will be used to provide additional constraints on our analysis. The inclusion of the DOZI amplitude, representing processes where the flavors in the final-state mesons are not correlated, provides a basis for calculating rates for $J/\psi\to\text{vector}+\text{gluonium}$ (θ or ι) and

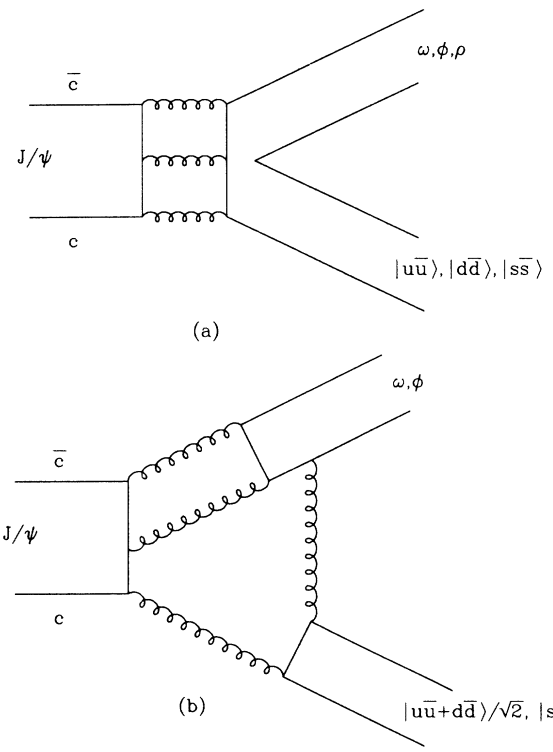

FIG. 1. Diagrams for strong J/ψ decays: (a) singly disconnected (SOZI) amplitude; (b) doubly disconnected (DOZI) amplitude.

TABLE I. Rates for $J/\psi \to \gamma +$ vector + vector.

VV state	Branching ratio: $J/\psi \to \gamma VV$ (Ref. 11)
$\omega\omega$	$1.76\pm0.09\pm0.45\times10^{-3}$
$\phi\phi$	$0.40\pm0.05\pm0.08\times10^{-3}$
$\omega\phi$	$0.14\pm0.025\pm0.028\times10^{-3}$

perhaps can provide insight into the odd pattern of rates in the axial-vector + vector sector. In our analysis we shall usually assume, below, that the η,η' are normal quark-antiquark states, and that the ι and θ are pure gluonium states. New, higher-statistics data from the Mark III experiment[14] on $P+V$ decays provide a much more stringent check of our model than the data previously available.

II. PSEUDOSCALAR + VECTOR FINAL STATES

A. The η-η' mixing angle

One crucial ingredient to the analysis is the quark content of the η and η'. We shall argue below that the data are consistent with the assumption that the dominant part of the η and η' wave functions consists solely of $u\bar{u}$, $d\bar{d}$, and $s\bar{s}$. Following Rosner,[3] we write

$$\eta = X_\eta \,|\, u\bar{u}=d\bar{d}\,\rangle/\sqrt{2} + Y_\eta \,|\, s\bar{s}\,\rangle \ ,$$
$$\eta' = X_{\eta'} \,|\, u\bar{u}+d\bar{d}\,\rangle/\sqrt{2} + Y_{\eta'} \,|\, s\bar{s}\,\rangle \ . \tag{1}$$

In terms of the singlet-octet mixing angle θ_P,

$$X_\eta = Y_{\eta'} = (\tfrac{1}{3})^{1/2}\cos\theta_P - (\tfrac{2}{3})^{1/2}\sin\theta_P = -\sin\alpha_P \ ,$$
$$X_{\eta'} = -Y_\eta = (\tfrac{1}{3})^{1/2}\sin\theta_P + (\tfrac{2}{3})^{1/2}\cos\theta_P = \cos\alpha_P \ . \tag{2}$$

Here $\alpha_P = \theta_P - \theta_I$, where $\theta_I \equiv \arctan(1/\sqrt{2}) = 35.3°$ is the ideal mixing angle. If we use the data for the two-photon width of the η,η' (Ref. 13), we can extract the following approximate values for the X's and Y's (see also Sec. II C):

$$X_\eta = 0.8, \quad Y_\eta = -0.6 \ ,$$
$$X_{\eta'} = 0.6, \quad Y_{\eta'} = 0.8 \ . \tag{3}$$

This corresponds to a singlet-octet mixing angle of about $\theta_P = -18°$, with no need for any gluonium admixtures. We show in Appendix A that this value for θ_P leads to a sensible pseudoscalar mass matrix.

Other determinations of these quantities are in good agreement with these values as summarized in Table II. Note that Table II contains a ratio of $J/\psi \to P+V$ rates which was not measured in Ref. 6. The J/ψ decays into $\rho\eta,\rho\eta'$ are electromagnetic and determine the η,η' quark content directly, subject to only small second-order corrections as outlined in Appendix B.

B. $P+V$ final state, simple model

In the Mark III paper[6] on $J/\psi \to P+V$ final states, two approaches were taken to look at the η,η' quark contents. The first used ratios of branching fractions, thereby avoiding assumptions about SU(3) violation, electromagnetic contributions, etc., which divide out. The second method used a detailed fit involving all of these contributing amplitudes. In this section we use an approach similar to the first method; however, we allow for a DOZI contribution. Since we will assume that the quark contents are given by Eq. (3) in Sec. II A, the ratios of J/ψ branching fractions $B(\omega\eta)/B(\rho^0\pi^0)$, $B(\omega\eta')/B(\rho^0\pi^0)$, and $B(\phi\eta')/B(\phi\eta)$ give three numbers which should be explainable in terms of one DOZI amplitude. Although we make a few simplifying assumptions, we get fairly reliable results. The more detailed analysis will be presented in Sec. II C.

In calculating the ratios of rates we take the DOZI amplitude to be $r\times$SOZI amplitude times a coupling factor depending on the flavor content of the final-state mesons. The coupling of the DOZI amplitude to $|\,u\bar{u}+d\bar{d}\,\rangle/\sqrt{2}$ is $\sqrt{2}$ times the coupling to $|\,s\bar{s}\,\rangle$. Hence the couplings for the diagram shown in Fig. 1(b) are

$$\sqrt{2}r(\sqrt{2}) \ \text{ for } \omega+ \,|\, u\bar{u}+d\bar{d}\,\rangle/\sqrt{2} \ ,$$
$$r(\sqrt{2}) \ \text{ for } \phi+ \,|\, u\bar{u}+d\bar{d}\,\rangle/\sqrt{2} \ , \tag{4}$$
$$\sqrt{2}r \ \text{ for } \omega+ \,|\, s\bar{s}\,\rangle, \quad r \ \text{ for } \phi+ \,|\, s\bar{s}\,\rangle \ .$$

TABLE II. Determinations of η,η' quark content.

Process	Prediction of simple model
$\dfrac{\sigma(\pi^- p\to\eta' n)}{\sigma(\pi^- p\to\eta n)} \Longrightarrow \left\lvert\dfrac{X_{\eta'}}{X_\eta}\right\rvert = 0.73\pm0.03$[a]	0.75
$\dfrac{B(J/\psi\to\rho\eta')}{B(J/\psi\to\rho\eta)} \Longrightarrow \left\lvert\dfrac{X_{\eta'}}{X_\eta}\right\rvert = 0.86\pm0.10$[b]	0.75
$\Gamma(\rho\to\gamma\eta) \Longrightarrow \lvert X_\eta\rvert = 0.71\pm0.09$[c]	0.80
$\Gamma(\phi\to\gamma\eta) \Longrightarrow \lvert Y_\eta\rvert = 0.61\pm0.06$[c]	0.60
$\Gamma(\eta'\to\gamma\rho) \Longrightarrow \lvert X_{\eta'}\rvert = 0.54\pm0.04$[c]	0.60
$\dfrac{B(J/\psi\to\gamma\eta)}{B(J/\psi\to\gamma\eta')} \Longrightarrow \theta_P = -22\pm2°$[d]	$-18°$

[a]Reference 15.
[b]Reference 14.
[c]Reference 16.
[d]Reference 9.

Potential phases between the SOZI and DOZI amplitudes are ignored, since any out-of-phase part will have a negligible effect in the rate. We have chosen to use ratios of rates for which both SU(3)-violating and electromagnetic terms are expected to cancel for the SOZI amplitudes (see Table IV below). We ignore, however, SU(3) violation in the DOZI amplitudes, since this will be of higher order in small quantities. Because the rates are given by $|\mathcal{M}|^2 p^3$, where $\mathcal{M}$ is the amplitude and p the vector momentum, we compare the reduced branching ratios $\tilde{B}=B/p^3$. The ratios of reduced rates are proportional to the squares of apparent wave function coefficients $X^{\rm eff}$ and $Y^{\rm eff}$, defined in Table III, which should reduce to the two-photon values if $r=0$. Adding the contributions from Figs. 1(a) and 1(b) gives the ratios shown in Table III.

The most striking feature of the data is the observed small value of $X^{\rm eff}_{\eta'}$. Taking $X^{\rm eff}_{\eta'}=0.25$ implies $r\simeq -0.15$. With a DOZI amplitude $r=-0.15$, we get the results of Table III.

Note that $r=0$, for which we expect $|X^{\rm eff}_{\eta'}|^2=0.36$, is completely excluded by the data.

C. $P+V$ final state, full calculation

We now proceed with a full calculation of the $P+V$ rates. A first-order parametrization of the amplitudes $\mathcal{M}$ is shown in Table IV. The notation is somewhat similar to that of Ref. 6. The more complete parametrization appears in Appendix B, and is described there in detail. In Table IV we make the approximation that all terms quadratic in small quantities are dropped. We again fit for the reduced branching ratio $\tilde{B}$, $\tilde{B}=B/p^3$, shown in the third column in units 10^{-3}. The J/ψ branching ratios B are from the Mark III experiment,[14] where common systematic errors due to the normalization have been taken out and remaining statistical and systematic errors added in quadrature. The data from DM2 (Ref. 17) are consistent with the Mark III values. We assume below ideal mixing for the vector mesons. That this is correct to the required precision is shown in Appendix C.

In Table IV the SOZI amplitude is g, the relative DOZI amplitude is r, s characterized the SU(3) violation, and e is the electromagnetic amplitude. The phase of e relative to g (denoted by θ_e) is also included in the fit. The data can be fit with various constraints in order to check various assumptions. We perform the following fits.

(1) Fully unconstrained fit to all variables in Table IV. In this case $X_\eta, Y_\eta, X_{\eta'}, Y_{\eta'}$ will not necessarily be related and need not saturate the η,η' wave function. This checks whether the J/ψ data alone can fix the mixing parameters. The result of this fit, which has one constraint, is given as the first fit in Table V. Using the numbers from the fit, we get $X^2_\eta+Y^2_\eta=1.00\pm0.16$ and $X^2_{\eta'}+Y^2_{\eta'}=1.44\pm0.25$. This result indicates that, using the J/ψ data alone, η and η' are both consistent with being normal quark states, consisting of $u\bar{u}$, $d\bar{d}$, and $s\bar{s}$ without other admixtures. The coefficients X and Y characterizing the quark content, however, still have rather large errors.

We are now in the position to check the necessity of including the DOZI amplitude. We do this by refitting the data requiring $r=0$. This fit results in $X^2_{\eta'}+Y^2_{\eta'}=0.41\pm0.09$ (similar to the original $P+V$ analysis),[6] but the probability of the fit is extremely low (4×10^{-6}): the χ^2 per degree of freedom is $\chi^2/{\rm DF}=25.1/2$. This confirms our conclusion in Sec. II B, that the DOZI amplitude must be included in the analysis. It is interesting to note that the main contribution to the χ^2 comes from the $\rho\eta'$ channel which, as mentioned earlier, measures $X_{\eta'}$ directly.

(2) To more fully constrain the fit values for $X_\eta, Y_\eta, X_{\eta'}, Y_{\eta'}$, we used as additional input[13,18] the two-photon width $\Gamma_{\gamma\gamma}$ of π^0,η,η',

$$\frac{\Gamma_{\gamma\gamma}(\eta)}{\Gamma_{\gamma\gamma}(\pi^0)}\left[\frac{m_{\pi^0}}{m_\eta}\right]^3=\frac{25}{9}\left|X_\eta+\frac{\sqrt{2}}{5}Y_\eta\right|^2$$

$$=1.07\pm0.07\ , \tag{5}$$

$$\frac{\Gamma_{\gamma\gamma}(\eta')}{\Gamma_{\gamma\gamma}(\pi^0)}\left[\frac{m_{\pi^0}}{m_{\eta'}}\right]^3=\frac{25}{9}\left|X_{\eta'}+\frac{\sqrt{2}}{5}Y_{\eta'}\right|^2$$

$$=1.63\pm0.08\ , \tag{6}$$

and the ratio of J/ψ radiative branching ratios into η and η' (Refs. 18 and 19):

$$\frac{B(J/\psi\to\gamma\eta)}{B(J/\psi\to\gamma\eta')}\left[\frac{p_{\eta'}}{p_\eta}\right]^3=\left|\frac{\sqrt{2}X_\eta+Y_\eta}{\sqrt{2}X_{\eta'}+Y_{\eta'}}\right|^2$$

$$=0.166\pm0.025\ . \tag{7}$$

These fits now have 4 degrees of freedom, yielding substantially smaller errors. At this stage we still do not impose any relations between the X's and Y's. The results are given as the second fit in Table V. We have neglected

TABLE III. Ratios of $J/\psi\to P+V$ rates, simple model.

Calculated with $r=-0.15$ and Eq. (3)	Data (Ref. 14)
$\frac{\tilde{B}(\omega\eta)}{\tilde{B}(\rho^0\pi^0)}=\lvert X^{\rm eff}_\eta\rvert^2\equiv\lvert X_\eta+\sqrt{2}r(\sqrt{2}X_\eta+Y_\eta)\rvert^2=0.48$	0.39 ± 0.06
$\frac{\tilde{B}(\omega\eta')}{\tilde{B}(\rho^0\pi^0)}=\lvert X^{\rm eff}_{\eta'}\rvert^2\equiv\lvert X_{\eta'}+\sqrt{2}r(\sqrt{2}X_{\eta'}+Y_{\eta'})\rvert^2=0.065$	0.050 ± 0.009
$\frac{\tilde{B}(\phi\eta')}{\tilde{B}(\phi\eta)}=\left\lvert\frac{Y^{\rm eff}_{\eta'}}{Y^{\rm eff}_\eta}\right\rvert^2\equiv\left\lvert\frac{Y_{\eta'}+r(\sqrt{2}X_{\eta'}+Y_{\eta'})}{Y_\eta+r(\sqrt{2}X_\eta+Y_\eta)}\right\rvert^2=0.69$	0.63 ± 0.12

TABLE IV. Parametrization and fit for $J/\psi \to P+V$.

Process	Amplitude $\mathcal{M}$	$\bar{B}(J/\psi \to P+V)\times 10^3$ Expt. (Ref. 14)	Fit
$\rho^+\pi^-,\rho^0\pi^0,\rho^-\pi^+$	$g+e$	1.556±0.161	1.306
$K^{*+}K^-,K^{*-}K^+$	$g(1-s)+e$	1.017±0.061	1.029
$K^{*0}\bar{K}^0,\bar{K}^{*0}K^0$	$g(1-s)-2e$	0.836±0.055	0.850
$\omega\eta$	$(g+e)X_\eta+\sqrt{2}rg(\sqrt{2}X_\eta+Y_\eta)$	0.632±0.058	0.639
$\omega\eta'$	$(g+e)X_{\eta'}+\sqrt{2}rg(\sqrt{2}X_{\eta'}+Y_{\eta'})$	0.079±0.010	0.083
$\phi\eta$	$[g(1-2s)-2e]Y_\eta+rg(\sqrt{2}X_\eta+Y_\eta)$	0.287±0.031	0.305
$\phi\eta'$	$[g(1-2s)-2e]Y_{\eta'}+rg(\sqrt{2}X_{\eta'}+Y_{\eta'})$	0.182±0.025	0.161
$\rho^0\eta$	$3eX_\eta$	0.071±0.010	0.090
$\rho^0\eta'$	$3eX_{\eta'}$	0.054±0.009	0.045
$\omega\pi^0$	$3e$	0.159±0.017	0.135
$\phi\pi^0$	0	<0.0026	

SU(3)-breaking effects in Eqs. (5)–(7). In fact such effects are rather small in the above ratios; a more complete analysis would not alter our results substantially.[20] For example, we can include nonet-symmetry-breaking effects in Eqs. (5) and (6) and fit for the ratio $R \equiv F_8/F_0$ where F_8 and F_0 are the octet- and singlet-decay constants.[20] Our fit yields $R=1.07\pm0.08$.

(3) Finally, we fit in terms of one quark sector mixing angle θ_P which relates the X's and Y's as shown in Eq. (2). The fit results are very consistent for the different sets of input data: $\Gamma_{\gamma\gamma}(\eta)$, $\Gamma_{\gamma\gamma}(\eta')$, and $B(J/\psi \to \gamma\eta)/B(J/\psi \to \gamma\eta')$ alone [Eqs. (5)–(7)]:

$$X_\eta=0.82\pm0.01,\quad \theta_P=-20°\pm1°,\quad \chi^2/\mathrm{DF}=9.4/2\ ;$$

$\Gamma_{\gamma\gamma}(\eta)$, $\Gamma_{\gamma\gamma}(\eta')$, $B(J/\psi \to \gamma\eta)/B(J/\psi \to \gamma\eta')$, and $P+V$ rates (Table IV):

$$X_\eta=0.82\pm0.01,\quad \theta_p=-20°\pm1°\ ,$$
$$r=-0.15\pm0.01,\quad \chi^2/\mathrm{DF}=19.9/7\ ;$$

$P+V$ rates (Table IV) alone:

$$X_\eta=0.81\pm0.01,\quad \theta_p=-19°\pm1°\ ,$$
$$r=-0.15\pm0.01,\quad \chi^2/DF=10.1/4\ .$$

The result of the latter fit is shown as the third fit in Table V. To compare fitted values with the data, we include the predicted reduced branching ratios $\bar{B}$ from this fit in Table IV.

As one can see, the results of the fits are very stable. The value for the DOZI amplitude is $r=-0.15\pm0.01$, identical to the result in the previous section. The SU(3)-breaking term s is small, equaling 10–20% of g. Allowing the DOZI amplitude r to have a phase $\theta_r \neq 0$ relative to g gives $r=-0.27\pm0.04$, $\theta_r=0.44\pm0.05$, and $X_\eta=0.75\pm0.03$ for the third fit in Table V.

We find that in most of the fits the $\rho\eta$ channel is contributing the largest amount to the χ^2, deteriorating the χ^2 probability of the fits. This channel is difficult to measure accurately because of ρ-ω interference. We have checked that the fit results are insensitive to whether or not this one channel is included.

D. Iota production, assuming it to be a glueball

The DOZI graph provides a direct way to produce glueballs with hadrons in J/ψ decay. The diagram is shown in Fig. 2, for the case of the ι, which is assumed to be a glueball.

To calculate the amplitude we need to know the relative coupling of the two-gluon system to the ι as compared to the η or η'. We estimate this by comparing ra-

TABLE V. $P+V$ fit results including DOZI.

	$P+V$	$\Gamma_{\gamma\gamma}(\eta),\Gamma_{\gamma\gamma}(\eta'),$ $\frac{J/\psi\to\gamma\eta}{J/\psi\to\gamma\eta'}$, and $P+V$	$P+V$ alone, one mixing angle
g	1.21±0.05	1.12±0.04	1.10±0.04
s	0.21±0.04	0.12±0.03	0.12±0.03
e	0.13±0.01	0.13±0.01	0.12±0.01
θ_e	1.26±0.11	1.26±0.11	1.25±0.12
r	−0.14±0.02	−0.14±0.01	−0.15±0.01
X_η	0.67±0.05	0.78±0.02	0.81±0.01
Y_η	−0.74±0.10	−0.53±0.04	
X'_η	0.58±0.06	0.54±0.02	
Y'_η	1.05±0.12	0.80±0.05	
χ^2/DF	0.02/1	10.5/4	10.1/4

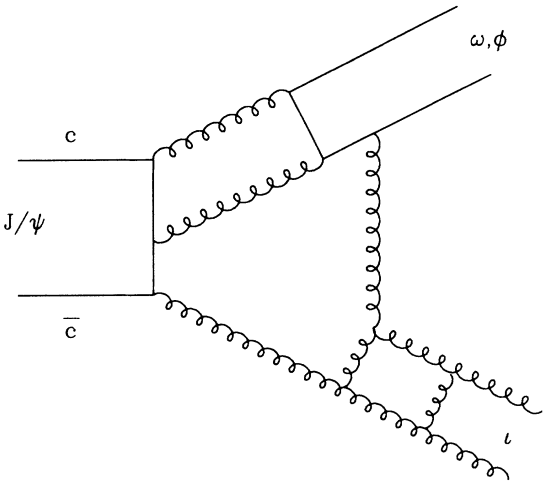

FIG. 2. Diagram for J/ψ decays into vector meson and glueball.

diative ι, η, and η' production using the rates for $J/\psi\to\gamma\eta$, $\gamma\eta'$, and $\gamma\iota$ which all are expected to occur via the two-gluon intermediate state as shown in Figs. 3(a) and 3(b). From the data[18] we learn that the rate for $\gamma+\iota$ is approximately equal to the sum of rates for $\gamma+\eta$ and $\gamma+\eta'$. Figure 2 suggests that it is a reasonable assumption that this observation continues to hold true for the DOZI diagram if the photon is replaced by a vector meson. This then normalizes the vector$+\iota$ final state relative to DOZI amplitudes for the $P+V$ final states previously studied. If we introduce a relative DOZI amplitude strength r' for $\phi+$gluonium [analogous to r in Eq. (4)], then the above normalization corresponds to $r'=\sqrt{3}r$. Coincidentally, one also finds $\sqrt{3}r$ for the relative DOZI amplitude for $\phi+\eta_1$ [where η_1 is the $q\bar{q}$ SU(3)-singlet pseudoscalar state], using Eq. (4). However, these two amplitudes are not related in an obvious manner. Using $r'=\sqrt{3}r$, one predicts the following rates in the approximation that the small electromagnetic term is ignored in the $\rho^0\pi^0$ calculation, no SU(3) breaking is included in the DOZI amplitudes, and $r=-0.15$ as determined in Sec. II C:

$$B(J/\psi\to\phi\iota)=(r')^2\left[\frac{p_\phi}{p_\rho}\right]^3 B(J/\psi\to\rho^0\pi^0)$$
$$=0.83\times10^{-4}\,,$$
$$B(J/\psi\to\omega\iota)=(\sqrt{2}r')^2\left[\frac{p_\omega}{p_\rho}\right]^3 B(J/\psi\to\rho^0\pi^0) \tag{8}$$
$$=2.4\times10^{-4}\,.$$

These rates may be compared to the Mark III (Ref. 21) 90%-confidence-level (C.L.) limit $B(J/\psi\to\phi\iota)\le 2.1\times10^{-4}$ and the ω E rate into $K\bar{K}\pi$ of $6.8^{+1.9}_{-1.6}\pm1.7\times10^{-4}$. In both cases of Eq. (8) the prediction for hadronic ι production is consistent with its nonobservation: the $\phi\iota$ upper limit is above the predicted rate and the observed ωE, being three times larger than the predicted $\omega\iota$ rate, might consist partly of $\omega\iota$.

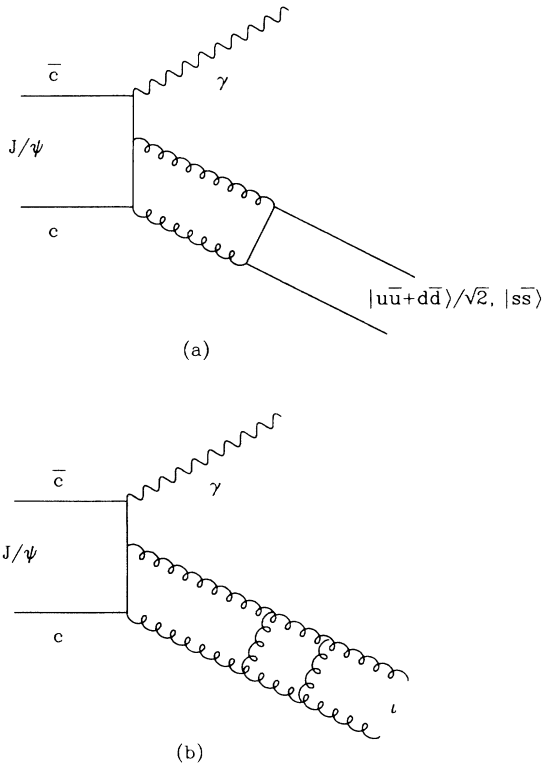

FIG. 3. Diagram for J/ψ radiative decays into (a) quark states, and (b) glueballs.

III. OTHER J/ψ TWO-BODY DECAYS

Since the pseudoscalar-vector data require a DOZI amplitude, we will now investigate the implications of such an amplitude for some of the other J/ψ two-body decays. Data here are much sketchier and our analysis is meant to point to how the DOZI amplitude can affect the decay pattern as well as stimulate further analysis of such decays.

A. Tensor + vector decays

It would be of interest to repeat the detailed analysis presented above for J/ψ decays into combinations of tensor and vector mesons. This would allow an independent check of the mixing for the f and f' and the possible glueball assignment for the θ. Unfortunately the data are more limited for these meson combinations. Even more important, because of the spins involved, a large number of parameters are needed to describe these decays. In the case of $J/\psi\to$ tensor+vector, there are five amplitudes needed to describe each decay. Each amplitude can, in principle, have a different amount of SU(3) violation, electromagnetic contribution, and DOZI contribution, where allowed. The phase-space variation is different for each of the five amplitudes, and also typically larger than in the case of the pseudoscalar-vector combinations.

A definition of the five amplitudes describing

$J/\psi \to T+V$ can be found in Ref. 22. In addition, an attempt to evaluate the variation of the branching ratios with the magnitude of the momentum in the J/ψ decay can be found in this reference. As an example, a factor of seven suppression of $\phi f'$ vs ωf due to kinematical factors was found, prior to any explicit SU(3) violation. This can account for most of the observed suppression of $\phi f'$ relative to ωf (Ref. 23) (see Table VI). Uncertainties in this factor, which depends on the admixture of amplitudes in the decay, can mask the presence of other phenomena such as explicit SU(3) violation or electromagnetic amplitudes.

Given these uncertainties, we will concentrate only on channels for which the phase-space correction is negligible, or those channels which are expected to be absent without tensor mixing or a DOZI amplitude. The latter channels are $\omega f', \phi f, \omega\theta, \phi\theta$. We will normalize the rates to the one for $\rho^0 A_2^0$, which is dominantly a SOZI strong decay analogous to $\rho^0\pi^0$ in the pseudoscalar-vector analysis. We will take for the f and f' a mixing pattern indicated by the two-photon widths,[13] which implies $X_f \simeq Y_{f'} \simeq 1$ and $Y_f \simeq 0.12, X_{f'} \simeq -0.12$, with an error of about ± 0.05.[24] With these wave functions we predict the relative rates shown in Table VI. They are exactly analogous to the parametrization of Table IV, if SU(3) violation and the electromagnetic amplitude are ignored. These amplitudes which we ignore would contribute corrections of the order of 15% to the terms in Table VI if their magnitude would be similar to the analogous terms in the $P+V$ case. In the table, we take r to be the relative DOZI amplitude for the quark-based states, and r' for the θ, assumed to be a glueball. We assume that the relative DOZI term is the same for each of the five amplitudes for a given $T+V$ decay. None of the channels in Table VI has an electromagnetic contribution in the absence of mixing of the tensors, except for ωf and ρA_2 which have identical amplitudes in the absence of a DOZI contribution. The relative amplitude r is normalized so that it is analogous to the same quantity for the quark-based pseudoscalar+vector final states in J/ψ decay.

Prior to looking at the results in Table VI, we will comment on some implications of the tensor mixing, since usually the tensors are approximated as an ideally mixed system ($Y_f = X_{f'} = 0$). The first expectation with nonideal mixing is that the f' should decay into $\pi\pi$. In the limit of flavor-SU(3)-nonet symmetry, we predict a ratio of branching ratios

$$\frac{B(f' \to \pi\pi)}{B(f' \to K\bar{K})} = \frac{3X_{f'}^2}{2(Y_{f'} + X_{f'}/\sqrt{2})^2} \left[\frac{p_\pi}{p_K} \right]^5 \simeq 0.096 , \quad (9)$$

using $X_{f'} = -0.12$. This will produce interference in the $\pi\pi$ channel with a prescribed phase (determined by the sign of $X_{f'}$) in reactions where both f and f' are produced, analogous to the expected f-f' interference in the $K\bar{K}$ channel. This phenomenon may have already been observed in $J/\psi \to \gamma\pi\pi$, where the f' appears as a shoulder on the f (Refs. 25 and 26). The negative sign of $X_{f'}$ correctly predicts the interference to be constructive for $\pi\pi$ masses between the f and f'. A similar effect has been seen in hadronic interactions.[27]

We list below other consequences of the nonideal mixing of f and f'.

(1) The ratio of radiative J/ψ branching fractions into f and f' is expected to be

$$\frac{B(J/\psi \to \gamma f')}{B(J/\psi \to \gamma f)} = \left| \frac{\sqrt{2}X_{f'} + Y_{f'}}{\sqrt{2}X_f + Y_f} \right|^2 \left[\frac{p_{f'}}{p_f} \right]^3 = 0.26 , \quad (10)$$

instead of the naive value of 0.5.

(2) There will be interference between the f and f' in $J/\psi \to \gamma\pi\pi$ or $\gamma K\bar{K}$. For masses between the f and f' the interference is constructive in the $\pi\pi$ channel and destructive for the $K\bar{K}$ channel.

(3) For $J/\psi \to \omega\pi\pi$ or $J/\psi \to \phi K\bar{K}$ both the production and decay amplitudes favor f in $\omega\pi\pi$ and f' in $\phi K\bar{K}$, such that these mass spectra are dominated by only one tensor meson each, in contrast with the radiative produc-

TABLE VI. Rates for $J/\psi \to$ tensor + vector.

Ratio of rates prior to phase-space correction[a] ($X_f \simeq Y_{f'} \simeq 1, X_{f'} = -Y_f = -0.12, r = 0.1, r' = 0.26$)	Ratio of decay momenta	Ratio of experimental rates[b,c]
$\frac{\omega f}{\rho^0 A_2^0} = \lvert X_f + \sqrt{2}r(\sqrt{2}X_f + Y_f) \rvert^2 = \lvert 1 + 2.16r \rvert^2 = 1.48$	1.015	1.4±0.18
$\frac{\omega f'}{\rho^0 A_2^0} = \lvert X_{f'} + \sqrt{2}r(\sqrt{2}X_{f'} + Y_{f'}) \rvert^2 = \lvert -0.12 + 1.17r \rvert^2 = 0$	0.89	<0.04 90%-C.L. limit
$\frac{\phi f'}{\rho^0 A_2^0} = \lvert Y_{f'} + r(\sqrt{2}X_{f'} + Y_{f'}) \rvert^2 = \lvert 1 + 0.83r \rvert^2 = 1.2$	0.77	0.23±0.06
$\frac{\phi f}{\rho^0 A_2^0} = \lvert Y_f + r(\sqrt{2}X_f + Y_f) \rvert^2 = \lvert 0.12 + 1.53r \rvert^2 = 0.07$	0.92	0.03±0.02
$\frac{\omega\theta}{\rho^0 A_2^0} = \lvert \sqrt{2}r' \rvert^2 = 0.14$	0.77	0.2±0.06
$\frac{\phi\theta}{\rho^0 A_2^0} = \lvert r' \rvert^2 = 0.068$	0.63	0.07±0.05

[a] $s = e = 0$ assumed below.
[b] Reference 21.
[c] Reference 23.

tion mentioned above. The interesting case of $J/\psi \to \omega K\bar{K}$ and $J/\psi \to \phi\pi\pi$ is discussed below.

(4) The mixing provides an excellent description of the tensor mass matrix, as discussed in Appendix A.

Returning to the predictions in Table VI, we look first at the ratio of branching ratios for ωf and $\rho^0 A_2^0$. This ratio will have the smallest phase-space dependence since the production momenta are nearly equal. In addition, in the absence of a DOZI amplitude, the ratio should be unity, even allowing for an electromagnetic term. A deviation from unity would indicate the presence of a DOZI amplitude. The present data in fact yield a result different from unity. Assuming a phase angle for r that is not too large, gives a value of $r \simeq 0.1$ which is roughly similar in magnitude to that found for the pseudoscalar + vector decays. Note, however, that the result requires the sign of r to be positive, which is opposite to the pseudoscalar + vector case.

Looking next at ϕf and $\omega f'$ in Table VI we see that they will have rates strongly effected by choosing the value of $r \simeq 0.1$, as found in the ωf case. In this case the mixing and DOZI terms add for ϕf and tend to cancel for $\omega f'$. Thus, instead of nearly equal rates as one might naively guess, the ϕf is enhanced by a factor of 4 in the rate, while the $\omega f'$ is reduced to nearly zero by the DOZI term. Better statistics for these two branching ratios are required to make a more quantitative comparison.

The results for θ production are of great interest because the θ is a glueball candidate. Including a reasonable phase-space correction, the relative rates for $\omega\theta$ and $\phi\theta$ are in good agreement with what is expected for a glueball, which couples to the singlet components of ω and ϕ. This contrasts strongly with the f and f', which are predominantly produced in a pattern dominated by the SOZI amplitude with nearly ideal mixing (e.g., $\omega f \gg \phi f$). Setting $|r'| = 0.26$ (i.e., simply taking the same value as used for the ι), would approximately reproduce the observed ratio of rates in Table VI if the phase-space correction needed to make the comparison to $\rho^0 A_2^0$ is not too great. It is not clear whether this is a good assumption, especially since the admixture of amplitudes for radiative or hadronic θ production is different from the analogous f or f' amplitudes.[22]

We mention finally that the $\phi\pi\pi$ is a particularly interesting channel. Based on our discussion of Table VI and tensor mixing, it should contain contributions of comparable size from ϕf, $\phi f'$, and $\phi\theta$: the f is produced with a small amplitude but decays with a large branching ratio into $\pi\pi$, the f' is produced with a large amplitude but decays via a small branching ratio, and the θ is produced and decays via a moderate amplitude and branching ratio. These three tensors should interfere with a phase which is determined by their quark content. In particular, we expect constructive interference for $\pi\pi$ masses between the f and f', arising from the opposite phase for $f \to \pi\pi$ and $f' \to \pi\pi$, as discussed earlier. For a glueball θ, we expect destructive interference for $\pi\pi$ masses between the f' and θ. Our expectation follows from the observed f'-θ interference seen in the $\phi K\bar{K}$ channel.[22] Since the interference is constructive in $\phi K\bar{K}$ for masses between the f' and θ, it will be destructive in the $\pi\pi$ case because the f' decay amplitude has changed sign, while the θ amplitude (assumed to behave like a singlet) is expected to not change sign when going from $K\bar{K}$ to $\pi\pi$.

B. Axial-vector + vector decays

This is the final set of multiplets on which new data exists. It is intermediate in complexity between $P+V$ and $T+V$ decays, being described by two invariant amplitudes. As shown in detail below, the observed pattern in the hadronic J/ψ decays is quite unusual and is difficult to explain without either large mixing and DOZI contributions or the assumption that states from different multiplets are observed in the data. Additional uncertainties arise from the poor understanding of the E decay channels. In this state of uncertainty we will assume below that the signals seen in the D and E mass region recoiling against the γ, ω, and ϕ are the normal $q\bar{q}$ axial vectors $D(1285)$ and $E(1420)$. This will tell us how far we can get assuming a minimal number of states. We note that an alternative choice for the $s\bar{s}$ axial vector has been presented in Ref. 28.

To begin the analysis we need to infer the quark contents of the mesons. We can again use the two-photon result[13,29] where the $D \to \eta\pi\pi$ and the $E \to K\bar{K}\pi$ are observed in off-shell production. Because the E branching ratio is not known, the data[30] reduce to

$$\frac{\Gamma_{\gamma\gamma}(E)}{\Gamma_{\gamma\gamma}(D)} = \frac{m_E^3}{m_D^3}\frac{(X_E+\sqrt{2}/5\,Y_E)^2}{(X_D+\sqrt{2}/5\,Y_D)^2} = \frac{0.34\pm0.18}{B(E\to K\bar{K}\pi)} . \tag{11}$$

Within $\pm 1\sigma$ deviations this gives a range of $X_E = 0.04 \to 0.43$ for a variation of the branching ratio $B(E\to K\bar{K}\pi) = 100\% \to 50\%$.

A second input is the data on radiative J/ψ decays from Mark III (Ref. 31) and DM2 (Ref. 17). While the D is observed in several channels, the signal for the E comes from $\eta\pi\pi$ only (mostly $\delta\pi$). Note that there is the interesting possibility that a signal of $E \to K\bar{K}\pi$ is hiding under what is summarily called the ι signal in radiative J/ψ decays to $K\bar{K}\pi$ (Ref. 32). Combining the D and E results gives the following relation:

$$\frac{B(J/\psi\to\gamma E)}{B(J/\psi\to\gamma D)} = \left[\frac{\sqrt{2}X_E+Y_E}{\sqrt{2}X_D+Y_D}\right]^2\left[\frac{p_E}{p_D}\right]^3 = \frac{0.85\pm0.25}{B(E\to\eta\pi\pi)} . \tag{12}$$

Allowing excursions of 1σ, changing the $\eta\pi\pi$ branching ratio $B(E\to\eta\pi\pi)$ from 10% to 50% changes X_E from 0.66 to 0.23. If we assume that $KK\pi$ and $\eta\pi\pi$ are the principal decay modes of the E, then the two data sets determine X_E and the branching ratios $B(E\to K\bar{K}\pi)$ and $B(E\to\eta\pi\pi)$ uniquely. Combining Eqs. (11) and (12), we get

$$X_E = 0.33^{+0.06}_{-0.11} , \quad B(E\to\eta\pi\pi) = 0.49^{+0.23}_{-0.10}, \quad B(E\to K\bar{K}\pi) = 0.51^{+0.10}_{-0.23} . \tag{13}$$

This result of relative large deviation from ideal mixing in the axial vectors and of a large $E\to\eta\pi\pi$ branching ratio is constrained by the following observations.

(1) Using the TPC upper limit on two-photon D production[13] we get, using Eqs. (11) and (12), $B(E\to\eta\pi\pi)<0.4$ for $X_E=0.33$.

(2) Mark II (Ref. 30) assumes $B(E\to\eta\pi\pi)=0$, i.e., $B(E\to K\bar{K}\pi)=1$. Then Eq. (11) yields $X_E=0.19^{+0.08}_{-0.15}$.

(3) $B(E\to\eta\pi\pi)$ is bounded by the Mark II upper limit $B(E\to\eta\pi\pi)/B(E\to K\bar{K}\pi)<0.6$ (Ref. 30).

(4) Mark III has analyzed the broad ι peak in the $K\bar{K}\pi$ mass spectrum from radiative J/ψ decays in terms of two resonances. The lower peak has the mass and width of the E (Ref. 32). Combining this $K\bar{K}\pi$ rate with the $\eta\pi\pi$ rate from Ref. 31, we get $B(E\to\eta\pi\pi)/B(E\to K\bar{K}\pi)=0.52\pm0.18$.

(5) Mark III observed $E\to\eta\pi\pi$ and $E\to K\bar{K}\pi$ in the hadronic channel $J/\psi\to\omega E$. The measured ratio is $B(E\to\eta\pi\pi)/B(E\to K\bar{K}\pi)=1.35\pm0.74$ (Ref. 31).

(6) WA76 (Ref. 33) and possibly GAMS (Ref. 34) have observed the $E\to\eta\pi\pi$ decay and their results are consistent with a large $E\to\eta\pi\pi$ decay width.

Taking all the above observations into account allows us to obtain a more reliable value for X_E. We shall take $B(E\to\eta\pi\pi)/B(E\to K\bar{K}\pi)=0.5\pm0.2$, and make use of Eqs. (11) and (12) to obtain

$$\begin{aligned} &X_E=0.35\pm0.10\ , \\ &B(E\to\eta\pi\pi)=0.33\pm0.09\ , \\ &B(E\to K\bar{K}\pi)=0.67\pm0.09\ , \end{aligned} \tag{14}$$

where the errors are estimated from the scatter of the data. We will use the mean of these values in the following. The D and E wave function are then

$$\begin{aligned} D&=0.94\,|\,u\bar{u}+d\bar{d}\,\rangle/\sqrt{2}-0.35\,|\,s\bar{s}\,\rangle\ , \\ E&=0.35\,|\,u\bar{u}+d\bar{d}\,\rangle/\sqrt{2}+0.94\,|\,s\bar{s}\,\rangle\ , \end{aligned} \tag{15}$$

where the relative signs of X_E and Y_E have been fixed by Eq. (11). The wave functions above imply that both D and E are produced in $\pi^-p\to(\eta\pi\pi)n$ and in $\pi^-p\to(K\bar{K}\pi)n$. In this case we predict

$$\frac{\sigma(\pi^-p\to En)}{\sigma(\pi^-p\to Dn)}=\left|\frac{X_E}{X_D}\right|^2=0.14\ . \tag{16}$$

In Appendix A, we discuss the axial-vector mass matrix. We note that in fact the large deviation from ideal mixing provides a more reasonable interpretation of the D and E masses than would the ideal mixing assumption.

We now turn to the hadronic J/ψ decays involving vector+axial-vector final states. In Table VII we show the amplitudes for $\omega D,\omega E,\phi D,\phi E$ including DOZI contribution r and SU(3)-breaking term s. To simplify the expression we leave out the electromagnetic amplitude, which had a small effect on the $P+V$ rates. We also include in Table VII the measured rates from Mark III (Ref. 21) and DM2 (Ref. 17), where we use $B(E\to K\bar{K}\pi)=0.67$, $B(E\to\eta\pi\pi)=0.33$. We corrected the experimental branching ratios by a kinematical factor which we took as p_V^5 in analogy to a detailed investigation of ϕ+tensor decays,[22] resulting in reduced branching ratios $\tilde{B}$. From a one-constraint fit to the data in Table VII we extract $g=4.0^{+0.6}_{-1.2}$, $s=0.36^{+0.05}_{-0.08}$, and $r=-0.35^{+0.13}_{-0.06}$. We include the calculated rates from the fit in Table VII. The errors do not include the uncertainty on the value of X_E and the E branching ratios, which we have shown are substantial. Using the value of g obtained above, we can predict the branching ratio $B(J/\psi\to\rho^0A_1^0)=3.2\times10^{-3}$, which is of the same magnitude as the J/ψ branching ratios into $\rho^0\pi^0$ (Ref. 14) and $\rho^0A_2^0$ (Refs. 17 and 23). Both the SU(3)-breaking term s and the DOZI amplitude r are about twice the value found in the $P+V$ case. We do not understand the origin of this difference. Note that the rates for ωD and ϕD are about the same size. These rates are independent of uncertainties in the E branching ratios and prove that mixing, the DOZI contribution and SU(3) breaking are important. The small rate for ϕE requires the DOZI term to be large and negative and the large rate for ωE requires both a negative DOZI term and a negative nonstrange component X_E. The observed pattern (Table VII)

$$\left[\frac{\tilde{B}(\omega D)}{\tilde{B}(\omega E)}\right]_{\text{expt}}=0.56\pm0.30,\quad \left[\frac{\tilde{B}(\phi D)}{\tilde{B}(\phi E)}\right]_{\text{expt}}>1.2 \tag{17}$$

is completely scrambled from the naive SOZI expectation ($r=0$, $s=0$), which would be

$$\begin{aligned} \left[\frac{\tilde{B}(\omega D)}{\tilde{B}(\omega E)}\right]_{\text{naive}}&=\left[\frac{X_D}{X_E}\right]^2=7.2\ , \\ \left[\frac{\tilde{B}(\phi D)}{\tilde{B}(\phi E)}\right]_{\text{naive}}&=\left[\frac{Y_D}{Y_E}\right]^2=0.14\ . \end{aligned} \tag{18}$$

IV. CONCLUSIONS

We have looked at a range of data on J/ψ decays in terms of a simple decay model incorporating both meson

TABLE VII. Rates for $J/\psi\to$axial vector+vector.

Channel	Amplitude[a] $X_E=-Y_D=0.35$, $Y_E=X_D=0.94$	$\tilde{B}(J/\psi\to A+V)\times10^4$ Expt. rate[b,c]	Fit
ωD	$g[X_D+\sqrt{2}r(\sqrt{2}X_D+Y_D)]=g(0.94+1.39r)$	4.6±2.1	3.3
ωE	$g[X_E+\sqrt{2}r(\sqrt{2}X_E+Y_E)]=g(0.35+2.03r)$	8.5±2.5	2.0
ϕD	$g[Y_D(1-2s)+r(\sqrt{2}X_D+Y_D)]=g[-0.35(1-2s)+0.98r]$	2.8±0.5	3.0
ϕE	$g[Y_E(1-2s)+r(\sqrt{2}X_E+Y_E)]=g[0.94(1-2s)+1.43r]$	<2.3	1.0

[a] $e=0$ assumed below.
[b] Reference 21.
[c] Reference 17.

mixing and the effect of doubly disconnected diagrams. For the case of the pseudoscalar mesons, the model gives good agreement with the quark wave functions determined from two-photon decays. We have extended the model to predict the rates in hadronic J/ψ decays into the glueball ι, which comes out smaller than present upper limits.

In the case of tensor+vector or axial-vector+vector decays, the model predicts a pattern of rates which is in general agreement with the data. Since the amplitudes can be extracted from the data, a much more definitive test will be possible once better measurements in more channels are available, providing constraints for the parametrization. The use of radiative J/ψ decays, as well as two-photon widths, should serve to determine the quark content of the axial vectors. Initial results, surprisingly, indicate that this multiplet is not ideally mixed. Better results in the case of the tensor mesons should serve to check more quantitatively our model assumptions and the assignment of the θ as a gluonium state.

ACKNOWLEDGMENT

This work was supported by the U.S. Department of Energy, Contract No. DE-AM03-76SF00010.

APPENDIX A: THE MESON MASS MATRIX

The pseudoscalar quark content allows us to calculate the mass matrix $\mathcal{M}$ for this case, assuming it is a two-state (η,η') system. The result in the basis given by $|u\bar{u}+d\bar{d}\rangle/\sqrt{2}$ and $|s\bar{s}\rangle$ is

$$\mathcal{M}=\begin{bmatrix} X_\eta^2 m_\eta + X_{\eta'}^2 m_{\eta'} & X_\eta Y_\eta m_\eta + X_{\eta'} Y_{\eta'} m_{\eta'} \\ X_\eta Y_\eta m_\eta + X_{\eta'} Y_{\eta'} m_{\eta'} & Y_\eta^2 m_\eta + Y_{\eta'}^2 m_{\eta'} \end{bmatrix} . \tag{A1}$$

Taking the results from Sec. II C, $X_\eta=0.81$, $Y_\eta=-0.58$, we get

$$\mathcal{M}=\begin{bmatrix} 0.66m_\eta+0.34m_{\eta'} & 0.47(m_{\eta'}-m_\eta) \\ 0.47(m_{\eta'}-m_\eta) & 0.34m_\eta+0.66m_{\eta'} \end{bmatrix} = \begin{bmatrix} 688 & 192 \\ 192 & 819 \end{bmatrix} \text{ MeV} . \tag{A2}$$

A simple model for this matrix, including SU(3) breaking is[35]

$$\mathcal{M}=\begin{bmatrix} m_\pi+2a^2 & \sqrt{2}ab \\ \sqrt{2}ab & m_{s\bar{s}}+b^2 \end{bmatrix} , \tag{A3}$$

where the mixing diagram is shown in Fig. 4. We associate an SU(3)-breaking factor $\sqrt{b/a}$ with each vertex containing strange-quark pairs. Using the numbers in Eq. (A2), we calculate $b^2=68$ MeV, $a^2=276$ MeV, and $m_{s\bar{s}}=751$ MeV. The value of $m_{s\bar{s}}$ serves to check the model since we can compare it to the value expected from other considerations. In a potential model, using one-gluon exchange,

$$\Delta=m(^3S_1)-m(^1S_0)=\tfrac{32}{9}\pi\alpha_s\frac{|\psi(0)|^2}{m_i m_j} , \tag{A4}$$

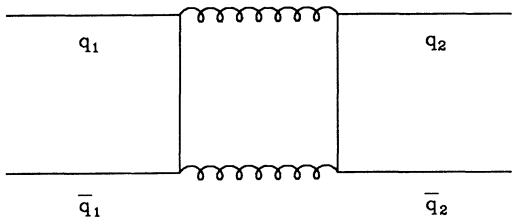

FIG. 4. Mixing diagram.

where m_i and m_j are the masses of the quarks making up the particular bound state. A range of predictions comes from assuming[36] (1) $\alpha_s|\psi(0)|^2$ constant, $\Delta=\text{const}/m_i m_j$, (2) α_s constant, $|\psi(0)|^2$ proportional to the reduced mass as for the case of linear potential, where $\Delta=\text{const}/(m_i+m_j)$.

These predict

$$m_{K^*}-m_K=\begin{cases} 0.60(m_\rho-m_\pi)=380 \text{ MeV} & \text{from (1)}, \\ 0.75(m_\rho-m_\pi)=470 \text{ MeV} & \text{from (2)}. \end{cases} \tag{A5}$$

The actual value is 400 MeV.

For the case in which we are interested, we get

$$m_\phi-m_{s\bar{s}}=\begin{cases} 0.6(m_{K^*}-m_K)=240 \text{ MeV} & \text{from (1)}, \\ 0.8(m_{K^*}-m_K)=320 \text{ MeV} & \text{from (2)}. \end{cases} \tag{A6}$$

Using the value of m_ϕ, this gives, for the mass of the $s\bar{s}$ pseudoscalar,

$$700\le m_{s\bar{s}}\le 780 \text{ MeV} , \tag{A7}$$

where above we have found $m_{s\bar{s}}=751$ MeV.

The agreement is very good and shows that a pseudoscalar mixing angle of $\theta_P=-19°$ is not contradicted by the mass matrix. A more general discussion of the mass matrix is given in Ref. 20. Note that a choice of $\theta_P=-10°$ does not result in a very different value for $m_{s\bar{s}}$, which shows that this is not a sensitive method for determining the mixing angle.

We can similarly look at the mass matrices for the isoscalar tensor and axial-vector mesons. We use the mixing pattern discussed in the text:[37]

$$\begin{aligned} &X_f=0.99, \quad Y_f=0.12, \quad X_{f'}=-0.12, \quad Y_{f'}=0.99 , \\ &X_D=0.94, \quad Y_D=-0.35, \quad X_E=0.35, \quad Y_E=0.94 , \end{aligned} \tag{A8}$$

to construct an experimentally determined mass matrix, as outlined in Eq. (A1). This matrix can then be analyzed using Eq. (A3) to extract what the masses of the $|u\bar{u}+d\bar{d}\rangle/\sqrt{2}$ and $|s\bar{s}\rangle$ mesons would be, if mixing did not exist. These masses can be compared to the known members of the appropriate octet for which mixing does not contribute. From Eq. (A1), we get

$$\begin{aligned} \mathcal{M}(2^+)&=\begin{bmatrix} 1276 & -30 \\ -30 & 1527 \end{bmatrix} \text{ MeV} , \\ \mathcal{M}(1^+)&=\begin{bmatrix} 1299 & 45 \\ 45 & 1402 \end{bmatrix} \text{ MeV} . \end{aligned} \tag{A9}$$

We note the difference in sign for the off-diagonal element in the two cases, with the sign for the axial vectors the same as in the pseudoscalar case, Eq. (A2). The relevance of this sign to understanding the mixing mechanism is discussed in Ref. 38. The off-diagonal element in the axial-vector matrix is small despite the large deviation from ideal mixing, due to the small value of $m_E - m_D$.

To extract a range of possible unmixed masses, which we indicate as $m(1^+), m(2^+)$ for the light-quark state and $m'(1^+), m'(2^+)$ for the $s\bar{s}$ state, we shall consider two extreme choices for the SU(3) violation in the mass matrix: one is perfect SU(3) symmetry in Eq. (A3), i.e., $a=b$, and the other the same degree of SU(3) violation as in the pseudoscalar case, i.e., $a=2b$. These give the following mass ranges, in MeV:

	$a=b$	$a=2b$
$m(2^+)$	1318	1355
$m'(2^+)$	1547	1537
$m(1^+)$	1236	1173
$m'(1^+)$	1434	1418

(A10)

For the tensors, the SU(3)-symmetric choice gives excellent agreement with expectations, which are the exact relation

$$m(2^+)=m_{A_2}=1318\pm 5 \text{ MeV} \tag{A11}$$

and the approximate relation

$$\tfrac{1}{2}[m(2^+)+m'(2^+)]=1433 \text{ MeV} \simeq m_{K_2^*(1430)} = 1426\pm 2 \text{ MeV} . \tag{A12}$$

Including the case of the axial vectors, where the SU(3) breaking is less well defined, we get, from Eqs. (A10), the following range of mass splittings:

$$\begin{aligned} &m'(2^+)-m(2^+)=229 \text{ MeV} , \\ &198 \le m'(1^+)-m(1^+) \le 245 \text{ MeV} , \\ &82 \le m(2^+)-m(1^+) \le 145 \text{ MeV} . \end{aligned} \tag{A13}$$

Thus the splitting between the two axial vectors is predicted to be similar to that of the two tensors, and the axial vectors are predicted to be lower in mass than the tensors by about 100 MeV.

These predictions are difficult to check since the masses of the octet axial-vector states A_1 and Q have some uncertainty. The cleanest place to study the A_1 is in τ decays. Results from different experiments[39] have now been consistently interpreted after allowance for the large A_1 width.[40] The resulting A_1 mass ranges from 1235±40 MeV to 1250±40 MeV, while the Particle Data Group[18] value is 1275±28 MeV, based primarily on hadronic scattering experiments. The value based on τ decays is in good agreement with the range of masses given in Eq. (A10). The mass of the strange axial-vector meson Q is difficult to determine because of mixing with the analogous 1^{+-} state. Extracted masses are $m_Q \simeq 1340$ MeV (Ref. 41) with values as low as $m_Q = 1310\pm 15$ MeV (Ref. 42). These are compatible with the predicted tensor–axial-vector splitting of approximately 100 MeV.

We note, finally, that the rather small splitting between the physical states D and E is caused primarily by the mixing pattern. This may be compared to the η'-η mass splitting which is even more reduced by mixing, compared to the $m_{s\bar{s}}$-m_π mass difference.

APPENDIX B: PARAMETRIZATION OF $J/\psi \to P + V$ AMPLITUDES

We parametrize the amplitudes of the decay $J/\psi \to P + V$ by the following terms: the SU(3)-symmetric SOZI amplitude g, the nonet-symmetry-breaking DOZI amplitude r, relative to g, and the electromagnetic amplitude e (with phase θ_e relative to g). The SU(3) violation is accounted for by a factor $(1-s)$ for every strange quark contributing to g, a factor $(1-s_p)$ for a strange pseudoscalar contributing to r, a factor $(1-s_v)$ for a strange vector contributing to r, and a factor $(1-s_e)$ for a strange quark contributing to e.

It is convenient to provide a translation of the formalism in Ref. 7 for the above parameters. In Ref. 7, a purely group-theoretical approach was used to obtain the matrix elements for the above amplitudes. Note that these arguments depend only on the assumption of flavor-SU(3) symmetry and its breaking due to a heavy-strange-quark mass and electromagnetic effects. In this sense, these results are independent of the detailed diagrams involved (shown in Figs. 1 and 5). In terms of the notation used in Ref. 7,

$$\begin{aligned} g &= g_8 + \frac{1}{\sqrt{3}} g_{m,88} , \\ sg &= \frac{\sqrt{3}}{2} g_{m,88} , \\ e &= \tfrac{1}{3} g_{e,88} , \\ rg &= \tfrac{1}{3}\left[g_1 - g_8 + \frac{1}{\sqrt{3}}(g_{m,81} + g_{m,18} - 2g_{m,88}) \right] , \\ rgs_p &= \frac{1}{\sqrt{3}}(g_{m,81} - g_{m,18}) , \\ rgs_v &= \frac{1}{\sqrt{3}}(g_{m,18} - g_{m,88}) . \end{aligned} \tag{B1}$$

For completeness, we have included in Table VIII a term which arises due to a combined mass/electromagnetic breaking of the flavor-SU(3) symmetry. This correction was first introduced by Isgur *et al.*[43] who analyzed corrections to $V \to P + \gamma$ radiative decays. They introduced a parameter $x \equiv \mu_d/\mu_s$ which accounts for the expected difference in the d-quark and s-quark magnetic moments due to mass breaking. It is easy to see that the $V \to P + \gamma$ amplitudes are precisely proportional to the electromagnetic contribution to the $J/\psi \to P + V$ decay, whose dominant decay occurs via $J/\psi \to \gamma \to P + V$. Thus we can simply read off the results of Ref. 43 and in-

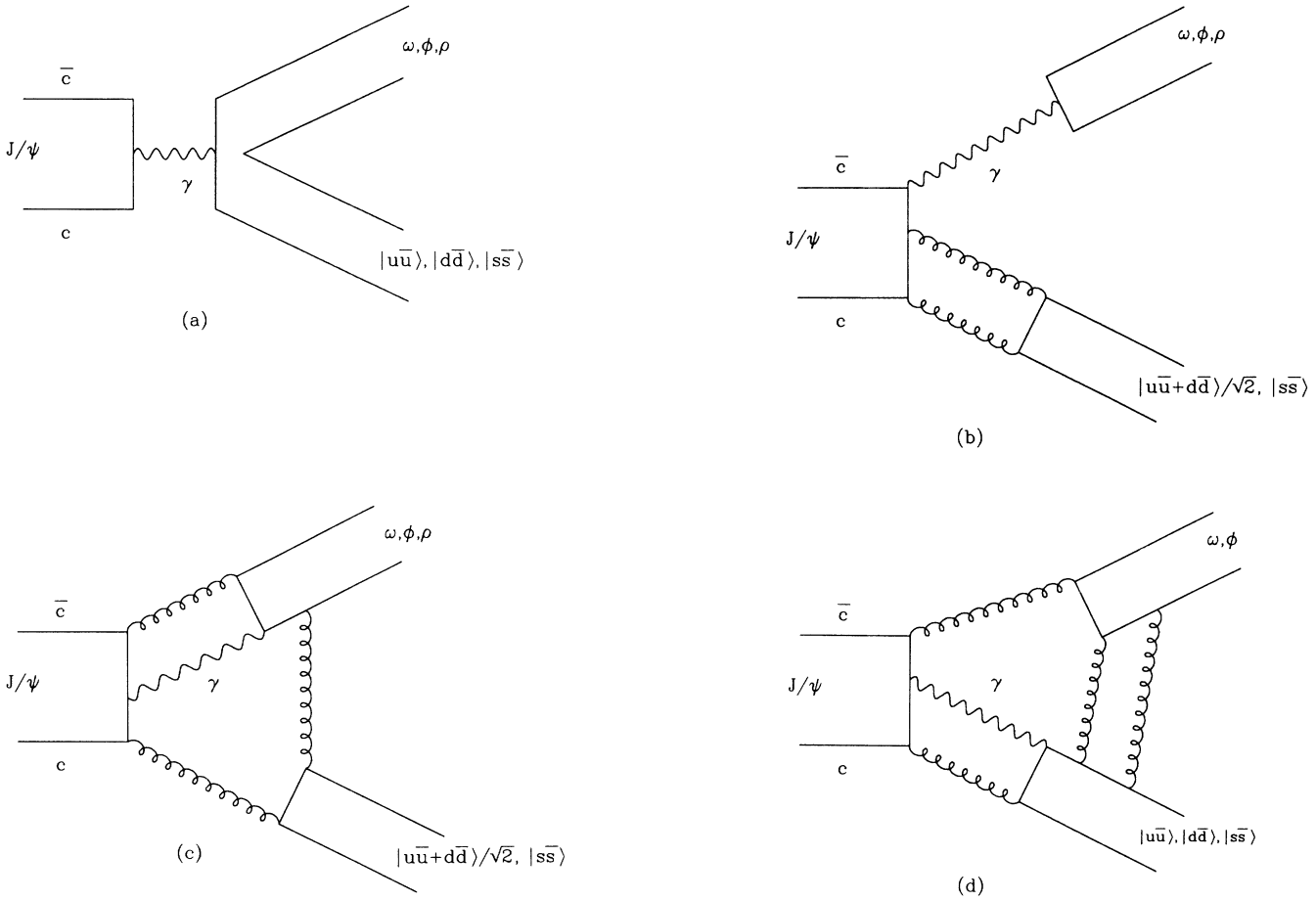

FIG. 5. Diagrams for electromagnetic J/ψ decays: (a) singly disconnected em amplitude; (b)–(d) doubly disconnected em amplitudes.

clude them in Table VIII. These results can be easily reproduced in the quark-model language by reducing the amplitude where the photon converts to an $s\bar{s}$ pair (as compared to an $u\bar{u}$ or $d\bar{d}$ pair) by a factor of $x \equiv 1-s_e$. It must be stressed that such a contribution represents only part of those terms which are second order in the SU(3)-symmetry breaking. For example, in quark-model language, we have yet to include symmetry breaking in the one-photon-exchange diagrams due to the production of $s\bar{s}$ quarks from the vacuum. As a result, including just some of the second-order contributions seems rather arbitrary. Including all of the second-order terms introduces too many new parameters to be of any utility. Hence, following Ref. 7, we have neglected all such terms in the analysis presented here.

In principle we should include corrections to the electromagnetic amplitude e equivalent to DOZI decays. However we expect that such corrections will be small. In order to present the argument, we show the electromagnetic graphs in Fig. 5 in the order of decreasing

TABLE VIII. General parametrization of amplitudes for $J/\psi \to P+V$.

Process	Amplitude
$\rho^+\pi^-,\rho^0\pi^0,\rho^-\pi^+$	$g+e$
$K^{*+}K^-,K^{*-}K^+$	$g(1-s)+e(1+s_e)$
$K^{*0}\bar{K}^{0},\bar{K}^{*0}K^0$	$g(1-s)-e(2-s_e)$
$\omega\eta$	$(g+e)X_\eta+\sqrt{2}rg[\sqrt{2}X_\eta+(1-s_p)Y_\eta]$
$\omega\eta'$	$(g+e)X_{\eta'}+\sqrt{2}rg[\sqrt{2}X_{\eta'}+(1-s_p)Y_{\eta'}]$
$\phi\eta$	$[g(1-2s)-2e(1-s_e)]Y_\eta+rg(1-s_v)[\sqrt{2}X_\eta+(1-s_p)Y_\eta]$
$\phi\eta'$	$[g(1-2s)-2e(1-s_e)]Y_{\eta'}+rg(1-s_v)[\sqrt{2}X_{\eta'}+(1-s_p)Y_{\eta'}]$
$\rho^0\eta$	$3eX_\eta$
$\rho^0\eta'$	$3eX_{\eta'}$
$\omega\pi^0$	$3e$
$\phi\pi^0$	0

importance. Figure 5(a) is the analogue to the SOZI amplitude [Fig. 1(a)], and Figs. 5(b)–5(d) are the analogues to the DOZI amplitude of Fig. 1(b), where Fig. 5(b) [Fig. 5(c), Fig. 5(d)] is suppressed by at least an additional factor α_s [α_s^2, α_s^3] relative to Fig. 5(a), respectively. The amplitude of Fig. 5(a) has flavor correlation in the final state and leads to $\{\rho,\omega\}+\pi$ and $\{\rho,\omega,\phi\}+\{\eta,\eta'\}$ final states. Figure 5(b) gives rise to $\{\rho,\omega,\phi\}+\{\eta,\eta'\}$, as does Fig. 5(c) which is a small correction to Fig. 5(b). Figure 5(d) is even more suppressed, but is the lowest-order diagram producing the $\pi^0+\phi$ final state: it leads to $\{\omega,\phi\}+\{\pi^0,\eta,\eta'\}$. We can estimate the relative size of these corrections to e from the data: Fig. 5(b) has as largest contributor $J/\psi\to\rho+\eta'$. Using the radiative J/ψ decay to η' and vector dominance as input, we get 1.1×10^{-5} for this DOZI electromagnetic rate, compared to an observed rate of 1.1×10^{-4}, a possible correction of 30% to the amplitude e. The diagram Fig. 5(d) can contribute to $J/\psi\to\pi^0+\phi$. Comparing the upper limit of $\tilde{B}<2.6\times10^{-6}$ for $\pi^0+\phi$ to the reduced branching ratio $\tilde{B}=1.6\times10^{-4}$ for $\pi^0+\omega$, one deduces that the amplitude of Fig. 5(d) contributes less than 20% of Fig. 5(a).

In order to simplify the expressions in Table VIII, we make use of the fact that e, r, s, s_ρ, and s_v are all small numbers and we therefore drop any product of those quantities when compared with g or unity. This results in Table IV, which will be compared to the data. The precision of the data[14] is in the best case about 6%, justifying that we ignore second-order correction terms.

APPENDIX C: LIMIT ON MIXING OF THE VECTOR MESONS

In our analysis above we have assumed that the vector mesons are ideally mixed to sufficient precision to ignore any vector mixing terms in the amplitudes. When using these amplitudes we kept terms of order 10%. Our approximations will therefore be valid provided we can show that the mixing is smaller than or of the order of a few percent. The most sensitive test of the mixing can be made in processes where there is interference between the strange and light quarks within a vector meson. Such a case is $\eta'\to\gamma\omega$, which can be normalized to $\eta'\to\gamma\rho$ where only the light quarks contribute. We take for η' the wave function $\eta'=0.58\,|\,u\bar{u}+d\bar{d}\,\rangle/\sqrt{2}+0.81\,|\,s\bar{s}\,\rangle$, as in our earlier analysis, while for the ω we take $\omega=X_\omega\,|\,u\bar{u}+d\bar{d}\,\rangle/\sqrt{2}+Y_\omega\,|\,s\bar{s}\,\rangle$. In order to proceed with the analysis, we must decide how to treat nonet-symmetry breaking. The most general formulas can be found in a review by O'Donnell.[44] In principle, two independent nonet symmetry-breaking parameters exist (called g_1 and g_1' in Ref. 44) corresponding to the two SU(3) nonets involved. To be as simple as possible, we will choose these parameters to be equal. Following our normalization exhibited in Eq. (B1), we introduce a parameter R defined by $Rg=\frac{1}{3}(g_1-g)$, where g is the SU(3)-invariant coupling constant. If we then take $X_\omega\approx1$ and $RY_\omega\approx0$ (anticipating a small deviation from ideal mixing for the vector mesons), we find

$$\frac{B(\eta'\to\gamma\omega)}{B(\eta'\to\gamma\rho)}=\frac{1}{9}\left|\frac{X_{\eta'}(1+4R)-2Y_{\eta'}\left[Y_\omega+\frac{R}{\sqrt{2}}\right]}{X_{\eta'}(1+2R)+\sqrt{2}RY_{\eta'}}\right|^2\frac{K_\omega}{K_\rho}\,. \tag{C1}$$

Here $K_\rho\propto k_\rho^3$, $K_\omega\propto k_\omega^3$ are kinematical factors integrated over the Breit-Wigner resonance of the ρ and ω, respectively, and thus are very sensitive to the exact parametrization of the Breit-Wigner shape. In Ref. 14 the resonance shape of the ρ was determined and we find $K_\omega/K_\rho=0.84\pm0.06$, where the error describes the uncertainty of the parametrization. Using the measured values $B(\eta'\to\gamma\rho)=(30.0\pm1.6)\%$ (Ref. 18) and $B(\eta'\to\gamma\omega)=(3.3\pm0.36)\%$ (Ref. 45) gives $Y_\omega=(-3.1\pm2.2)\%$ for $R=0$. Using instead the Particle Data Group (PDG) value $B(\eta'\to\gamma\omega)=(2.7\pm0.5)\%$ (Ref. 18) gives $Y_\omega=(0.6\pm3.0)\%$. The uncertainty in the ρ line shape contributes an additional systematic error of $\pm1.5\%$. We cannot determine Y_ω and R simultaneously. For the branching ratio of Ref. 45, setting $Y_\omega=0$ gives $R=-0.037$. Taking $R=\pm0.1$ gives $Y_\omega=-0.11$ and $Y_\omega=0.05$, respectively.

Thus, provided R is small, the deviation from ideal mixing in the vector mesons is less than or of the order of a few percent in the amplitude, and can be ignored in our analysis. Note, finally, that a mass-matrix calculation for the vector mesons following the procedure in Appendix A would yield a similar conclusion.

[1] J. D. Bjorken, in *Proceedings of the International Europhysics Conference on High Energy Physics,* edited by A. Zichichi (CERN, Geneva, 1979), p. 245.

[2] M. S. Chanowitz, in *Proceedings of the IXth SLAC Summer Institute on Particle Physics,* edited by A. Mosher (SLAC, Stanford, 1982), p. 41.

[3] J. L. Rosner, Phys. Rev. D **27**, 1101 (1983).

[4] In order to facilitate the reading, we are making use of the traditional particle names. In terms of the official PDG names, we use f for $f_2(1270)$, A_2 for $a_2(1320)$, f' for $f_2'(1525)$, θ for $f_2(1720)$, A_1 for $a_1(1270)$, Q for $K_1(1280)$, D for $f_1(1285)$, E for $f_1(1420)$, and ι for $\eta(1440)$.

[5] S. Okubo, Phys. Lett. **5**, 165 (1963); G. Zweig (unpublished); J. Iizuka, Prog. Theor. Phys. Suppl. **37-38**, 21 (1966).

[6] R. M. Baltrusaitis *et al.*, Phys. Rev. D **32**, 2883 (1985).

[7] H. E. Haber and J. Perrier, Phys. Rev. D **32**, 2961 (1985).

[8] An early look at the J/ψ two-body reactions was done by G. Gidal (private communication).

[9] A. Seiden, in *Proceedings of the VII International Workshop on Photon-Photon Collisions,* edited by A. Courau and P. Kessler (World Scientific, Singapore, 1986).

[10] S. S. Pinsky, Phys. Rev. D **31**, 1753 (1985); A. Bramon and J.

Casulleras, Z. Phys. C **32**, 467 (1986).

[11]G. Eigen, in *Proceedings of the XVII International Symposium on Multiparticle Dynamics,* Seewinkel, Austria, 1986, edited by M. Markytan, W. Majerotto, and J. MacNaughton (World Scientific, Singapore, 1987).

[12]J. C. Sens, in *Physics in Collision V,* proceedings of the 5th International Conference, Autun, France, 1985, edited by B. Aubert and L. Montanet (Editions Frontières, Gif-sur-Yvette, France, 1986).

[13]J. Olsson, *Proceedings of the XXIIIth International Symposium on Lepton and Photon Interactions at High Energies,* Hamburg, Germany, 1987, edited by Wulfrim Bartel and Beinhold Ruckl [Nucl. Phys. B Proc. Suppl. **3** (1988)].

[14]D. Coffman *et al.*, Report No. SLAC-PUB-4424 (unpublished).

[15]W. D. Apel *et al.*, Phys. Lett. **83B**, 131 (1978); N. R. Stanton *et al.*, *ibid.* **92B**, 353 (1980). The value quoted is for the ratio of nonflip amplitudes. From the ratio of spin-flip amplitudes, one gets 0.82 ± 0.01 from both experiments when using the integrated cross section.

[16]J. L. Rosner, in *Proceedings of the 1985 International Symposium on Lepton and Photon Interactions at High Energies,* Kyoto, Japan, 1985, edited by M. Konuma and K. Takahashi (Research Institute for Fundamental Physics, Kyoto University, Kyoto, 1986).

[17]J. E. Augustin *et al.*, LAL ORSAY Report No. LAL 85-27, 1985 (unpublished); G. Szklars *et al.*, in *Hadron '87,* proceedings of the Second International Conference on Hadron Spectroscopy, Tsukuba, Japan, 1987, edited by Y. Oyanagi, K. Takamatsu, and T. Tsuru (KEK, Tsukuba, 1987), p. 96.

[18]Particle Data Group, M. Aguilar-Benitez *et al.*, Phys. Lett. **170B**, 1 (1986).

[19]The PDG value used agrees with a new, more precise value of the DM2 experiment (F. Couchot, Thèse de Doctorat, LAL 87-55, 1987).

[20]F. Gilman and R. Kauffman, Phys. Rev. D **36**, 2761 (1987).

[21]J. J. Becker *et al.*, Phys. Rev. Lett. **59**, 186 (1987).

[22]R. Xu, Ph.D. thesis, University of California, Santa Cruz, SCIPP Preprint 87/108, 1987.

[23]L. Köpke, in *Progress in Electroweak Interations,* Vol. 1 of proceedings of the XXI Rencontre de Moriond, Les Arcs, France, 1986, edited by J. Tran Thanh Van (Editions Frontières, Gif-sur-Yvette, France, 1986); U. Mallik, in *Strong Interactions and Gauge Theories,* Vol. 2 of proceedings of the XXI Rencontre de Moriond, p. 431.

[24]As a sign convention, we choose that the X_i of the predominantly light quark state and the Y_i of the predominantly strange-quark state are set close to $+1$. Obviously, the results are independent of this choice.

[25]R. M. Baltrusaitis *et al.*, Phys. Rev. D **35**, 2077 (1987).

[26]J.-E. Augustin *et al.*, Z. Phys. C **36**, 369 (1987).

[27]V. Chabaud *et al.*, Acta Phys. Pol. B **12**, 575 (1981); A. Pawlicki *et al.*, Phys. Rev. D **15**, 3196 (1977).

[28]D. Aston *et al.*, Phys. Lett. **201B**, 573 (1988); P. Gavillet *et al.*, Z. Phys. C **16**, 119 (1982).

[29]G. Gidal, in *Proceedings of the VII International Workshop on Photon-Photon Collisions,* edited by A. Courau and P. Kessler (World Scientific, Singapore, 1986); H. Aihara *et al.*, Phys. Rev. Lett. **57**, 2500 (1986).

[30]G. Gidal *et al.*, Phys. Rev. Lett. **59**, 2012 (1987); **59**, 2016 (1987).

[31]J. J. Becker *et al.*, Report No. SLAC-Pub-4246, 1987 (unpublished).

[32]W. Wisniewski *et al.*, in *Hadron '87* (Ref. 17).

[33]T. A. Armstrong *et al.*, in *Hadron '87* (Ref. 17).

[34]T. Mouthuy *et al.*, in *Proceedings of the International Europhysics Conference on High Energy Physics,* Bari, Italy, 1985, edited by L. Nitti and G. Preparata (Laterza, Bari, Italy, 1985).

[35]A. De Rújula, H. Georgi, and S. L. Glashow, Phys. Rev. D **12**, 147 (1975).

[36]M. Frank and P. J. O'Donnell, Phys. Lett. **159B**, 174 (1985).

[37]In terms of the convention of Ref. 13,

$$X_f=0.99,\ Y_f=0.12,\ X_{f'}=0.12,\ Y_{f'}=-0.99,\ \theta_T=28^\circ,$$

$$X_D=0.94,\ Y_D=-0.35,\ X_E=-0.35,\ Y_E=-0.94,\ \theta_A=56^\circ.$$

[38]J. F. Donoghue, in *Antiproton Proton Physics and the W Discovery,* proceedings of the XVIII Rencontre de Moriond, La Plagne, France, 1983, edited by J. Tran Thanh Van (Editions Frontières, Gif-sur-Yvette, France, 1983).

[39]W. Ruckstuhl *et al.*, Phys. Rev. Lett. **56**, 2132 (1986); W. B. Schmidke *et al.*, *ibid.* **57**, 527 (1986); H. Albrecht *et al.*, Z. Phys. C **33**, 7 (1986).

[40]M. G. Bowler, Phys. Lett. B **182**, 400 (1986); N. A. Tornqvist, in *Hadrons, Quarks and Gluons,* proceedings of the XXII Rencontre de Moriond, edited by J. Tran Thanh Van (Editions Frontières, Gif-sur-Yvette, France, 1987).

[41]R. K. Carnegie *et al.*, Phys. Lett. **68B**, 287 (1977).

[42]C. Daum *et al.*, Nucl. Phys. **B187**, 1 (1981).

[43]N. Isgur *et al.*, Phys. Rev. Lett. **36**, 1262 (1976).

[44]P. J. O'Donnell, Rev. Mod. Phys. **53**, 673 (1981).

[45]D. Alde *et al.*, Yad. Fiz. **45**, 1341 (1987) [Sov. J. Nucl. Phys. **45**, 830 (1987)].